ELSEVIER

Marine Geology 190 (2002) 95–118

MARINE GEOLOGY
INTERNATIONAL JOURNAL OF MARINE GEOLOGY, GEOCHEMISTRY AND GEOPHYSICS

www.elsevier.com/locate/margeo

Deltas south of the Bosphorus Strait record persistent Black Sea outflow to the Marmara Sea since ~10 ka

R.N. Hiscott [a,*], A.E. Aksu [a], D. Yaşar [b], M.A. Kaminski [c], P.J. Mudie [d], V.E. Kostylev [d], J.C. MacDonald [a], F.I. Işler [b], A.R. Lord [c]

[a] *Department of Earth Sciences, Memorial University of Newfoundland, St. John's, NF, Canada A1B 3X5*
[b] *Institute of Marine Sciences and Technology, Dokuz Eyül University, Haydar Aliyev Caddesi No. 10, Inciralı, Izmir 35340, Turkey*
[c] *Department of Geological Sciences, University College London, Gower Street, London WC1E 6BT, UK*
[d] *Geological Survey of Canada – Atlantic, P.O. Box 1006, Dartmouth, NS, Canada B2Y 4A2*

Received 12 May 2001; accepted 19 February 2002

Abstract

At the southern exit of the Bosphorus Strait in the northeastern Marmara Sea, high-resolution seismic profiles reveal two lobate, progradational delta lobes in modern water depths of ~40–65 m. The younger delta was active from ~10 to 9 ka based on radiocarbon dates of equivalent prodelta deposits and the elevation of its topset-to-foreset transition. The topset-to-foreset transition climbs in the seaward direction because the delta prograded into a rising sea. Low abundances of marine fauna and flora in the 10–9-ka interval support a deltaic interpretation. There are no rivers in the area that could have fed the delta; instead, all evidence points to the strait itself as the source of sediment and water. When this outflow was strongest (~10.6–6.0 ka), sapropels accumulated in basinal areas of both the Aegean and Marmara seas. Benthic foraminiferal and dinoflagellate cyst data from contemporary deposits elsewhere in the Marmara Sea point to the continual presence through the Holocene of a surface layer of brackish water that we ascribe to this same outflow from the Black Sea through the Bosphorus Strait. By ~9.1–8.5 ka, two-layer flow developed in the Bosphorus Strait as global sea level continued to rise, and the sediment supply to the younger delta was cut off because the outflowing Black Sea water ceased to be in contact with the floor of the strait. The older delta lobe lies below a prominent lowstand unconformity and is tentatively interpreted to have formed from ~29.5 to 23.5 ka (oxygen-isotopic stage 3) when the Marmara Sea stood at ~−55 m and a second sapropel accumulated in deep basinal areas.

Keywords: Marmara Sea; Black Sea; transgression; deltas; sequence stratigraphy

1. Introduction

The Marmara Sea is an oceanographic link (a 'gateway') between the world's largest permanently anoxic basin, the Black Sea, and the Aegean Sea of the eastern Mediterranean basin (Fig. 1). It is connected to the Black Sea and the Aegean Sea through the straits of Bosphorus (~40 m deep) and Dardanelles (~70 m deep), respectively. The sill depth in the Dardanelles was greater in the past (e.g. ~75 m at 12 ka; ~105 m at

* Corresponding author. Fax: +1-709-737-2589.
E-mail address: rhiscott@sparky2.esd.mun.ca (R.N. Hiscott).

0025-3227/02/$ – see front matter
PII: S0025-3227(02)00344-4

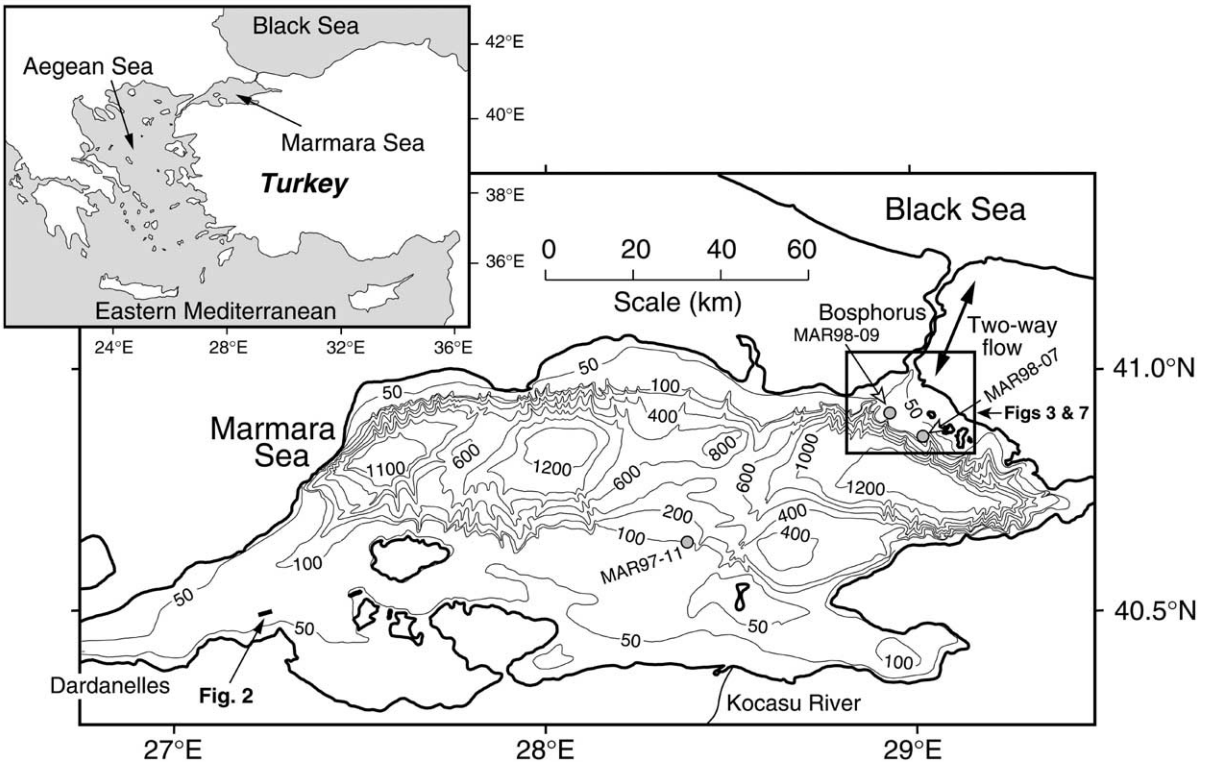

Fig. 1. Bathymetry of the Marmara Sea (isobaths in meters) and the narrow connection to the Black Sea through the Bosphorus Strait. Origin of the deep basins is discussed by Aksu et al. (2000). The inset map shows the entire gateway area from the Aegean Sea in the SW to the Black Sea in the NE. The focus of this paper is a strategic area just south of the Marmara Sea exit from the Bosphorus (box labelled as Figs. 3 and 7).

125 ka) because of persistent tectonic uplift of the region around the strait by ~0.40 mm/yr (Yaltırak et al., 2002). The present water exchange across the Bosphorus is a two-layer flow (Latif et al., 1992). A cooler (5–15°C) and lower salinity (17–20‰) surface layer exits the Black Sea at 10–30 cm s^{-1}. Warmer (15–20°C) and higher salinity (38–39‰) Mediterranean water flows northward through the strait, at depth, with velocities of 5–15 cm s^{-1} (Özsoy et al., 1995; Polat and Tuğrul, 1996). There is a net water export of ~300 km^3 yr^{-1} from the Black Sea because fresh-water input from large rivers, combined with precipitation onto the sea surface, exceeds evaporation. This exported volume, at about 50% normal marine salinity, is ~50 times the cumulative annual discharge of the largest rivers entering the Marmara Sea along its southern margin (Aksu et al., 1999, their fig. 4).

Satellite altimetry shows that the surface of the Black Sea is, on average, 30 cm (±10 cm) above the level of the Marmara Sea (Beşiktepe et al., 1994). The Marmara Sea, in turn, is approximately 5–27 cm above the level of the northern Aegean Sea (Bogdanova, 1969). These elevation differences represent hydraulic heads that drive the net outflow into the Aegean Sea via the straits of Bosphorus and Dardanelles.

In the western Marmara Sea, earliest Holocene barrier islands, sand waves and current-generated marine bars are entombed beneath a widespread veneer of marine mud that accumulated after the sand bodies were drowned by sea-level rise and colonized by algal–serpulid bioherms (e.g. Fig. 2). Cross stratification in the current-generated deposits indicates unidirectional west-directed flow that Aksu et al. (1999) attributed to post-glacial export of low-salinity water from the Black

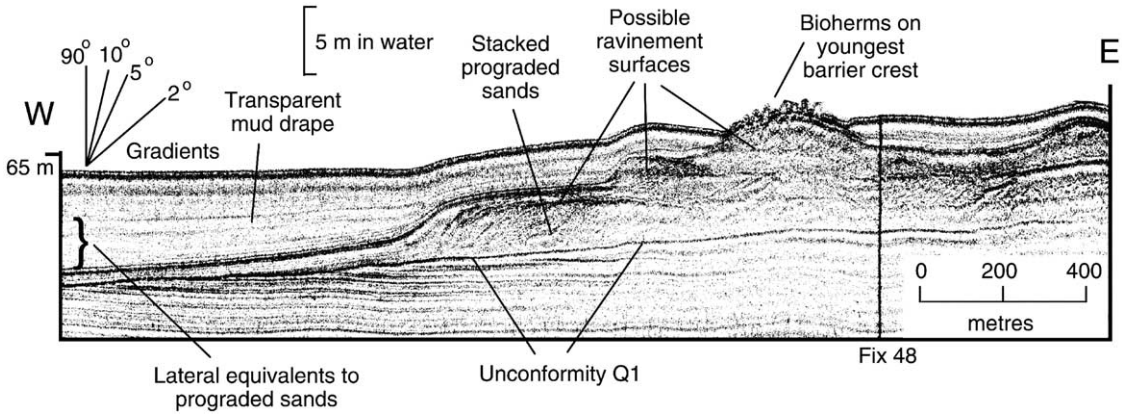

Fig. 2. Huntec DTS profile from the western Marmara Sea (location in Fig. 1) showing stratified, prograded, acoustically reflective sediment mounds overlying an angular unconformity and underlying a widespread mud drape. The mounds are interpreted by Aksu et al. (1999) as barrier islands abandoned during the rapid Holocene transgression. Note the basal onlap of the drape and the local lateral transition between the base of the drape and the barrier-island sands. Small rough elements on the crest of the youngest barrier are algal–serpulid bioherms (Aksu et al., 1999) that have radiocarbon ages as old as 9850 ± 70 yr BP (Iso-Trace TO-7779).

Sea, starting at ~9.6 ka and ending at ~6.5–7.0 ka. Their conclusion was supported by multi-proxy climatic and oceanographic data from Aegean Sea cores, which provide evidence for a ~10°C rise in sea-surface temperature and a 1.0–1.5‰ decrease in sea-surface salinity at the start of the Holocene (Aksu et al., 1995a,b). Continued outflow of brackish water into the Aegean Sea provided a low-salinity surface lid, which prevented vertical mixing and ventilation, thus promoting the deposition, between ~9.6 and ~6.4 ka, of the most recent sapropel S1 in the Aegean Sea (Aksu et al., 1995a,b). More recent coring in the Marmara Sea indicates that sapropel deposition began earlier there, at ~10.6 ka (Çağatay et al., 2000; Aksu et al., 2002a), and by inference the onset of Black Sea outflow might have been earlier than previously thought by about 1000 yr. Palynological data from Marmara and Black Sea cores also show that brackish-water (~7–12‰) dinoflagellate cyst assemblages were present prior to and at the onset of sapropel deposition (Mudie et al., 2001, 2002a).

The conclusions of Aksu et al. (1995a,b; 1999) and Mudie et al. (2002a) are in direct conflict with a view of Black Sea history published by Ryan et al. (1997) and Ryan and Pitman (1998), and widely disseminated in television documentaries and in a number of articles in popular science magazines and newspapers (Mastel, 1997; McInnis, 1998; Brown, 1999). Ryan et al. (1997) suggested that the early Holocene Black Sea was a giant fresh-water lake standing at −150 m, and that it was catastrophically flooded at ~7.15 ka by Mediterranean water when the Bosphorus Strait was breached during the last phases of post-glacial global sea-level rise. Ryan and Pitman (1998) linked this proposed rapid flooding of the Black Sea shelves to Noah's Flood as chronicled in the Old Testament. Increasingly, new results from the Black Sea and Marmara Sea challenge this hypothesis of catastrophic flooding (Çağatay et al., 2000; Görür et al., 2001; Mudie et al., 2001, 2002b).

Airgun profiles acquired in 1995 (lines shown in Aksu et al., 1999, their fig. 2) suggested the presence of prograded sediment bodies just south of the Bosphorus Strait in the northern Marmara Sea. In this area, the 100-yr significant storm wave height is approximately 3.6 m, with corresponding significant wavelength and period of 82 m and 7 s, respectively (Institute of Marine Sciences and Technology, unpublished database). Hence, the shelf is wave-influenced to depths of ~40 m. The area where progradational sediment bodies occur was selected for detailed follow-up

studies during subsequent cruises in 1998 and 2000, leading to the recognition and mapping of two lobate deposits, interpreted as deltas, at present water depths of ~40–65 m on the wave-dominated shelf. These deltas, particularly the youngest one, are the focus of this paper. They are of critical importance in adjudicating the incompatible interpretations of Aksu et al. (1999) and Ryan et al. (1997).

2. Data acquisition and approach

High-resolution boomer profiles were collected in 1998 and 2000 along ~280 km of tracks in the northern Marmara Sea, just south of the exit of the Bosphorus Strait (Fig. 3A). Track spacing was 2–3 km to allow mapping of the deposits. These surveys used a Huntec Deep Towed System (DTS) with a 500-J broad-band source, recorded using a 21-element, 6-m-long Benthos hydrophone streamer. The Huntec DTS profiles have a vertical resolution of 15–30 cm, and locally provide details on sedimentary deposits up to 50–100 m below the seabed. Bathymetry (Fig. 3B) was digitized every 10 min (~1.85 km at a survey speed of 6 knots) from 12 kHz echo-sounder records. GPS navigational fixes were taken every 10 min. Throughout this paper, two-way travel times are converted to depths below sea level using an interval velocity of 1500 m s^{-1}, which has been found to be appropriate for both the water column and near-surface siliciclastic sediments in open-marine conditions (e.g. Emeis et al., 1996).

A number of gravity cores were collected using a 4-m-long, 400-kg corer with 10-cm internal diameter (for complete core inventory, see Aksu et al., 2002a). Six key cores were identified, in which critical stratigraphic horizons determined in seismic profiles could be studied and dated. These cores were systematically subsampled for micropaleontological and stable isotopic studies. Approximately 20 cm^3 of sediment was removed at 10-cm intervals from each core. For planktonic foraminiferal and coccolith studies, samples were wet-sieved through a 63 μm-screen. The coarse fraction was dried in an oven at 40°C, weighed and dry-sieved through a 125-μm screen. Plank-

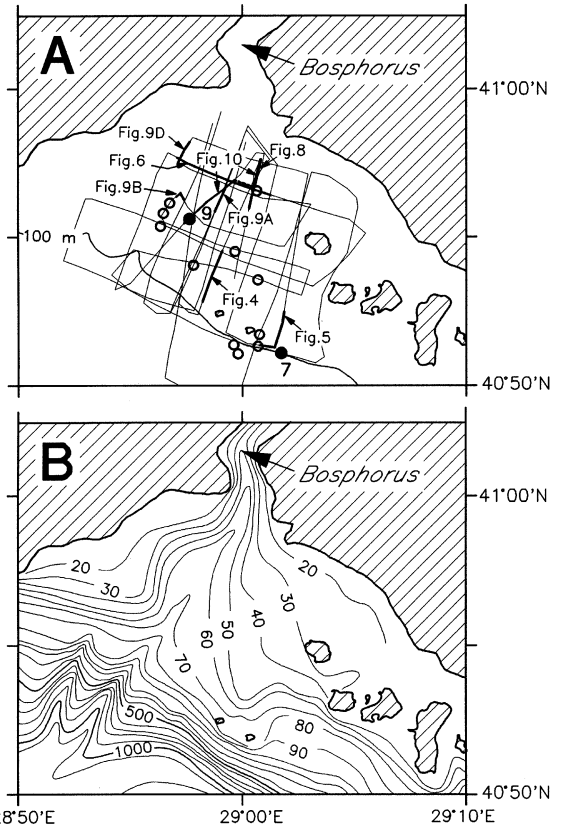

Fig. 3. Maps of the study area south of the Bosphorus exit (see Fig. 1 for location). (A) Index map showing the location of ~280 line-km of boomer survey tracks and gravity cores (open circles for cores not discussed in this paper; solid circles for cores MAR98-07 and -09). Heavy lines are Huntec DTS profiles illustrated in Figs. 4–6 and 8–10. (B) Bathymetry with contours each 10 m above −100 m depth and each 100 m below −100 m depth.

tonic foraminifera were identified and counted in each >125-μm fraction using the taxonomic descriptions of Saito et al. (1981) and Kennett and Srinivasan (1983). Subsequently, all species counts were converted to percentages. Benthic foraminifera were picked from >125-μm fractions; their taxonomy is discussed by Kaminski et al. (2002). For coccolith studies, the <63-μm fractions were wet-sieved through a 20-μm cloth; <2-μm fractions were further separated out using a centrifuge. Coccoliths were identified and counted in the 20–2-μm fractions in all the key cores using the taxonomic descriptions of Kleijne (1993) and

Table 1
Core locations, water depths, and radiocarbon dates

Core number	Latitude (N)	Longitude (E)	Water depth (m)	Fix number	Reference figure	Radiocarbon age (yr BP)	Shell depth (cm)	IsoTrace Lab number	Calendar age (cal BP)
MAR97-11	40°39.20′	28°22.67′	111	1 684.1	Aksu et al. (1999) their fig. 12	10 790 ± 70	79	TO-7774	12 000 ± 630
						12 970 ± 80	92	TO-7775	14 400 ± 500
						14 940 ± 90	174	TO-7776	17 400 ± 565
						15590 ± 90	204	TO-7777	18 150 ± 600
MAR98-07	40°50.98′	29°00.98′	95	874.6	Fig. 3	15 210 ± 100	72	TO-7785	17 650 ± 600
						43 550 ± 790	95	TO-8454	NA
						41 480 ± 610	119	TO-7786	NA
						41 900 ± 610	180	TO-7787	NA
						40 460 ± 590	217	TO-7788	NA
MAR98-09	40°55.36′	28°56.80′	64	920.7	Figs. 3 and 10	4 500 ± 60	35	TO-7789	4 650 ± 145
						6 120 ± 70	42	TO-8455	6 540 ± 160
						8 810 ± 100	52	TO-8456	9 400 ± 330
						9 070 ± 70	60	TO-7790	9 700 ± 430
						9 840 ± 80	94	TO-7791	10 850 ± 460
						10 220 ± 70	113	TO-7792	11 200 ± 500

Radiocarbon ages have no reservoir correction, and are based on a half life of 5568 yr. Errors represent 68.3% confidence limits. Calibrated calendar ages were calculated using OxCal (Stuiver et al., 1998a,b), a marine reservoir correction of 415 yr (Marine Reservoir Correction Database, Queens University, Belfast, Ireland), and include 95% confidence limits based on graphical scatter about a best-fit line relating radiocarbon ages and tree-ring ages. A listing of all radiocarbon dates in the Marmara Sea is available in Aksu et al. (2002a).

Winter and Siesser (1994). Palynological methods are documented elsewhere (Mudie et al., 2001, 2002b).

Gastropod and bivalve shells were extracted from split cores, and identified under the guidance of co-author Kostylev with the help of a number of reference texts for Mediterranean molluscs (Mordukhai-Boltovskoi, 1972; Abbott and Dance, 1998; Poppe and Goto, 1991, 1993). Selected shell samples were radiocarbon-dated at the IsoTrace Radiocarbon Laboratory of the University of Toronto. The dates are the average of two separate analyses and are corrected for natural and sputtering fractionation to a base of $\delta^{13}C = -25‰$. Before hydrolysis, the outer 20–35% of the shell samples was removed by HCl leaching to ensure that clean, unaltered carbonate was analyzed. Calibrated calendar ages with a reservoir correction of 415 yr are presented in Table 1, but ages reported in the text are uncalibrated with no reservoir correction.

3. Seabed physiography and seismic units

Southwest of the Bosphorus Strait, a prominent submarine canyon dissects the Marmara Sea shelf edge (Fig. 3B). Shelf width is greater east of the canyon (10–15 km) than to the west (3–5 km). The shelf-slope break occurs at ~90 m water depth, with very steep slopes (15–20°) leading to the floor of the easternmost deep basin of the Marmara Sea at ~1200 m (Fig. 1; Basin 3 of Aksu et al., 2000).

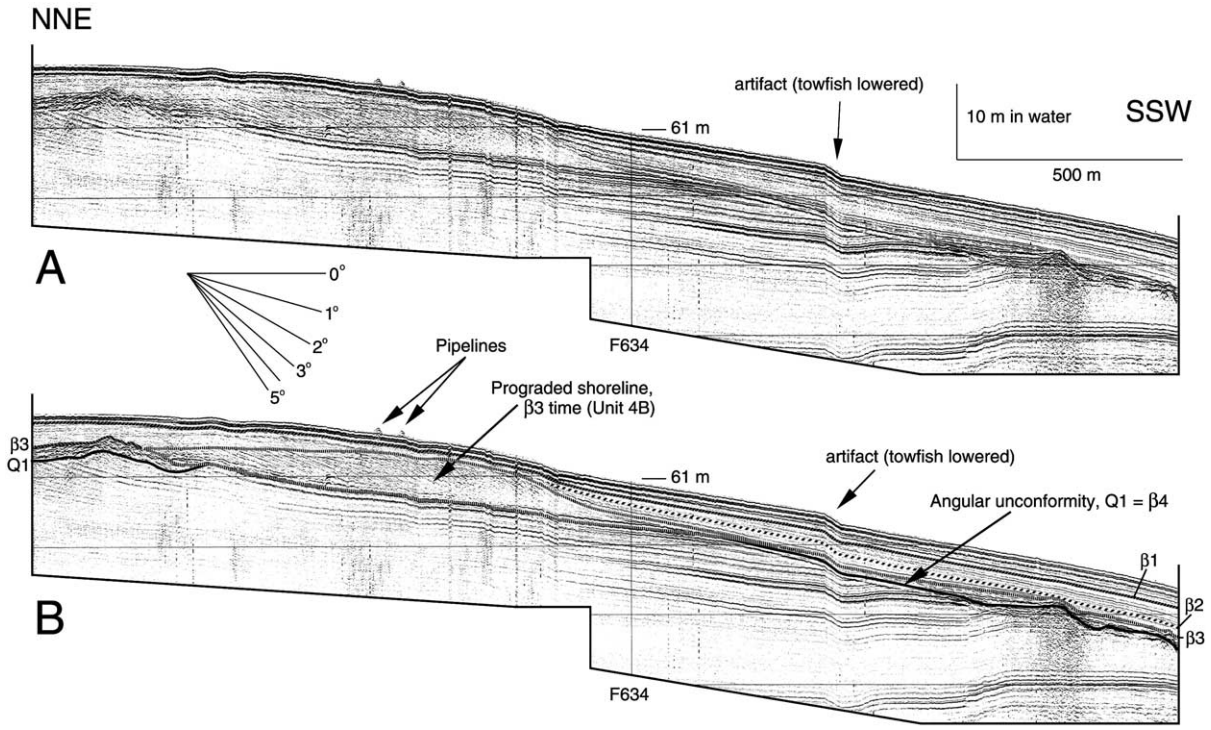

Fig. 4. Unmarked and interpreted Huntec DTS profile near the shelf edge south of the Bosphorus Strait (location in Fig. 3A), showing a prominent angular unconformity, Q1, that elsewhere underlies latest Quaternary shelf muds and prograded sediment packages (Fig. 8). Sediments below the unconformity have inferred ages of >160 ka. There is an areally restricted bench of prograded clinoforms in Subunit 4B, interpreted as a beach/shoreline deposit dating from oxygen-isotopic stage 2 (22–12 ka). Deposits above this bench are inferred to be younger than ~11 ka.

3.1. Unit boundaries

The latest Quaternary succession on the shelf east of the canyon lies above a prominent reflection along which underlying units are sharply truncated. This is an erosional, angular unconformity that we designate Q1 (Fig. 4). Where cored (see 4.3. Core MAR98-07), Q1 truncates deposits with a minimum age exceeding ~40 ka; we argue later (5.1. Chronology) that these deposits are most likely older than ~160 ka, and that the prolonged isotopic stage 6 lowstand (~−100 m for ~35 000 yr; Skene et al., 1998) produced unconformity Q1. Although beyond the scope of this paper, our boomer profiles show several earlier episodes of shelf-wide erosion (unconformities Q2 to Q4, Fig. 5), best seen near the shelf edge, that presumably formed during earlier glacial lowstands.

Above unconformity Q1, the latest Quaternary succession is divisable into five seismic–stratigraphic units (Units 1–5) which are separated from one another by shelf-wide reflectors β1, β2, β3 and β4, all younger than Q1 (Fig. 6). β1 underlies Unit 1, β2 underlies Unit 2, and so on (Table 2). Q1 underlies Unit 5 except near the shelf edge where Units 4 and 5 are locally missing because of depositional thinning; in this area, Q1 merges with β3 and β4, and is overlain directly by Unit 3 (Fig. 5). The four β reflectors are unconformities characterized by subtle erosional truncation of underlying deposits and local downlap or onlap of overlying deposits. β3 is different from the rest in that it is commonly a surface of marked low-angle and step-wise truncation of underlying reflectors. Hiscott and Aksu (2002) define basin-wide allostratigraphic units in the Marmara Sea; their allostratigraphic Subunits A1 and A2 corre-

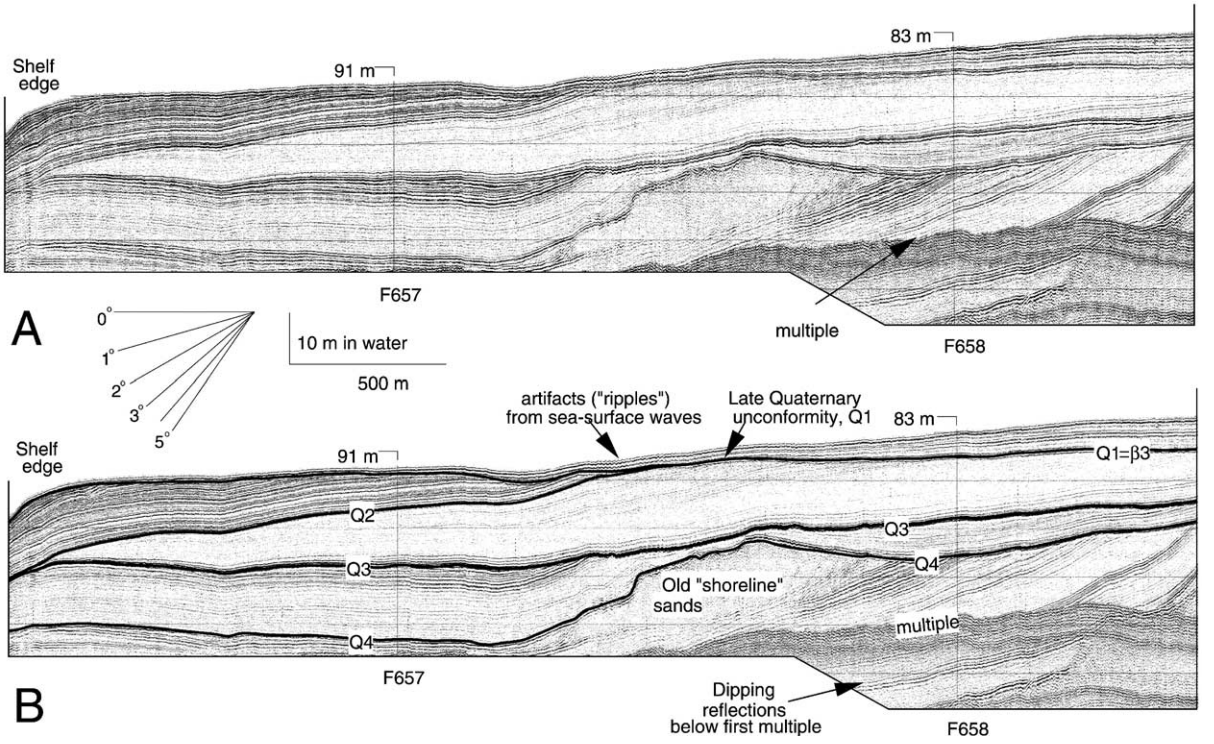

Fig. 5. Unmarked and interpreted Huntec DTS profile near the shelf edge south of the Bosphorus Strait (location in Fig. 3A), showing four prominent shelf-crossing unconformities (Q1–Q3) that are interpreted as subaerial erosion surfaces formed during major lowstand events. Q3 is an angular unconformity landward of an inferred sandy shoreline wedge (beach or barrier-island sands), and is a conformable surface farther offshore. Here, near the shelf edge, β3 and β4 are coincident with Q1 at the resolution of the seismic profiles so that most deposits above Q1 are younger than ~11 ka.

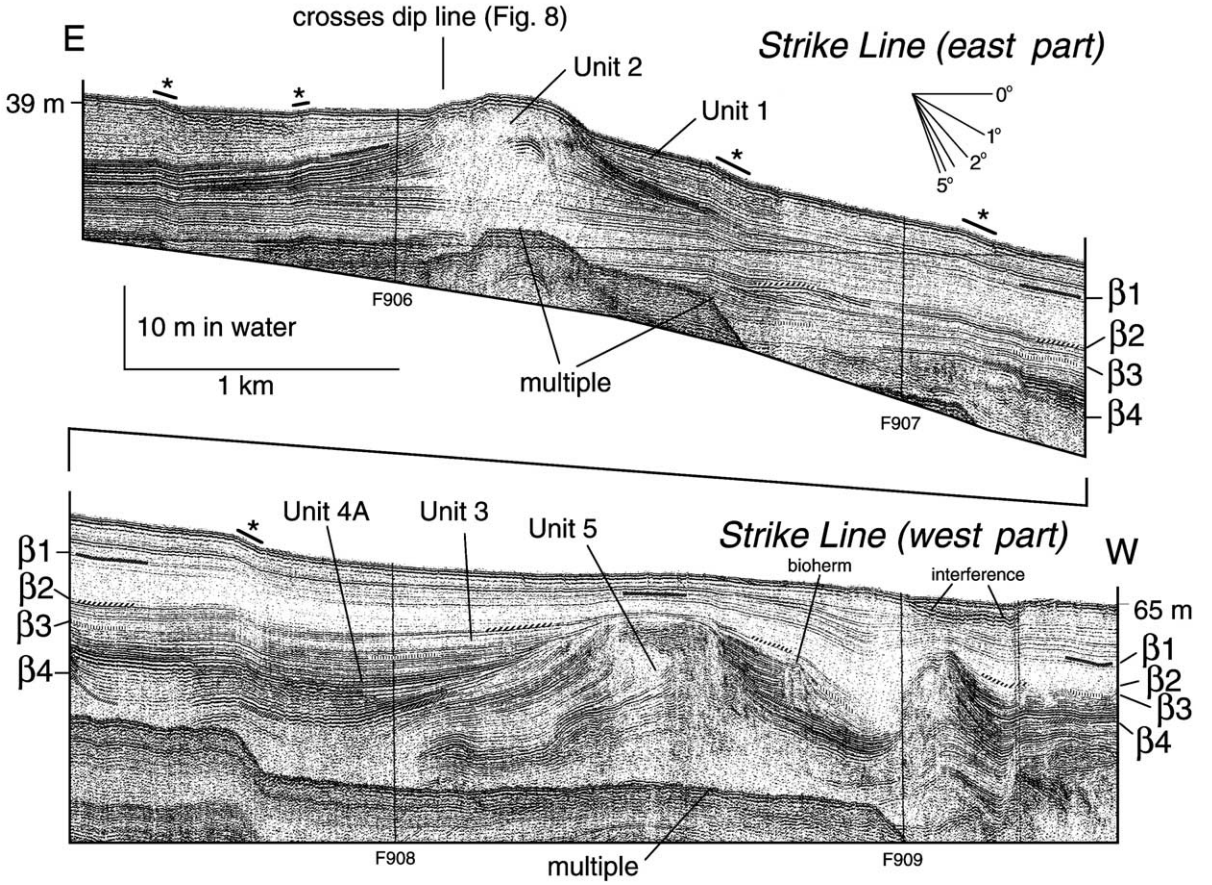

Fig. 6. Huntec DTS profile across two prominent south-prograded depositional lobes of Unit 2 and Unit 5 south of the Bosphorus Strait (location in Fig. 3A). Bold bars beneath * signs mark places where raising or lowering of the Huntec towfish created apparent steps in the seafloor. Units 1, 3, and Subunit 4A fill inter-lobe depressions and onlap the deltaic lobes. Regional unconformities β1–β4 are marked intermittently to permit their tracing across the profile, and are discussed in the text. This seismic profile crosses the profile in Fig. 8, as indicated.

spond to Units 1–3 of this paper, whereas their allostratigraphic Unit B corresponds to Units 4 and 5.

3.2. Descriptions of seismic units

The youngest Unit 1 is a regularly reflective package of weak to moderate, continuous reflectors, which show clear onlap onto β1 around highs of the underlying Unit 2. Unit 1 is thickest (~12 ms, or ~9 m) beneath the central eastern shelf and rapidly thins to <1 ms near the shelf break.

Below Unit 1 is a south-prograded lobate depositional sequence (Unit 2, Fig. 7A). In dip profiles crossing the thickest part of the depositional lobe, Unit 2 exhibits an oblique prograded seismic configuration where clinoforms terminate updip by toplap and erosional truncation at β1 (Fig. 8), and downdip by downlap onto β2. The depth to the top of individual clinoforms climbs upward in the direction of progradation, with the top of the youngest clinoform situated at a depth of about −40 m below modern sea level (Fig. 8). In strike profiles (Fig. 6), the prograded unit forms a mound beneath which reflections converge both east and west toward the margin of the mound.

Table 2
Stratigraphic units, bounding surfaces, and chronology

Unit	External form	Reflection configuration	Age	Interpretation or comments
1	Seaward-thinning wedge, onlapping fill	Weak to moderate, continuous reflections	9–0 ka	Shelf muds below storm wave base
	------β1------		9 ka	Onlap surface over abandoned delta lobe
2	Lobate mound passing distally into seaward-thinning wedge	Weak to moderate, dipping clinoforms passing distally to seaward-converging continuous reflections	10–9 ka	Delta lobe supplied by Black Sea outflow
	------β2------		10 ka	Downlap surface for Unit 2 delta lobe
3	Seaward-thinning wedge, onlapping fill	Weak to moderate, continuous reflections, local wedges of clinoforms, local mounds at base	*12*–10 ka	Shelf muds, local prograded shelf wedges, algal–serpulid bioherms at base, local infill of erosional relief on β3
	------β3------		*22–12 ka*	Lowstand erosional surface of last glacial maximum (oxygen-isotopic stage 2), possible outer shelf ravinement surface
4B	Wedge-shaped, flat-topped bench toward outer shelf	Weak to moderate reflections, dipping clinoforms thinning distally to a rapid pinchout	*?15–12 ka*	Lowstand (or early transgressive) shoreline sands and silts (shoreface), passes laterally into β3 and may be its time equivalent
4A	Seaward-thinning wedge, onlapping fill	Weak to strong, continuous to locally irregular reflections	*23.5–22 ka*	Shelf silts and muds with minor reworked shelf sands
	------β4------		*23.5 ka*	Onlap surface over abandoned delta lobe
5	Lobate mound passing distally into seaward-thinning wedge, local mid-shelf mounds	Weak to moderate reflections, dipping clinoforms passing distally to low-angle clinoforms and irregular scour-and-fill geometries	*29.5–23.5 ka*	Delta lobe supplied by Black Sea outflow, mid-shelf reworked sands and muds
	------Q1------		*160–125 ka*	Major lowstand angular unconformity truncating a variety of older deposits

Ages in italics are inferred (see text) whereas those in normal font are based on radiocarbon dates.

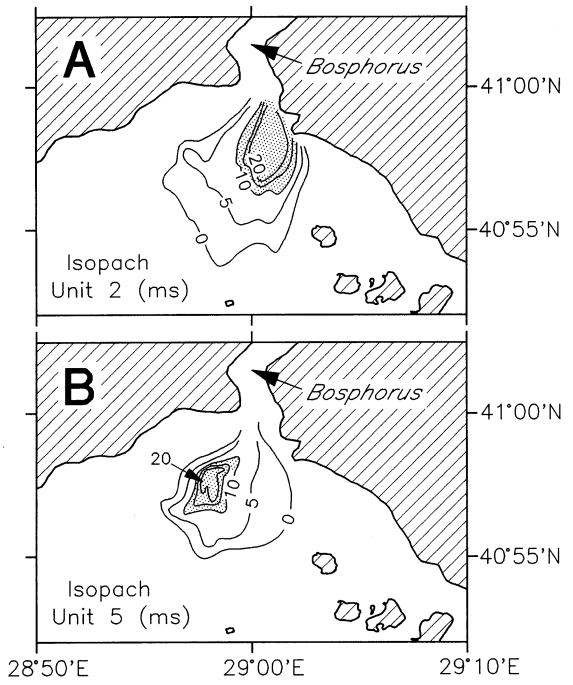

Fig. 7. Isopach maps of Unit 2 and Unit 5 depositional lobes (A and B, respectively), showing sediment thicknesses in milliseconds of two-way travel time, where 10 ms ≈ 7.5 m.

Unit 3 is separated from the overlying Unit 2 by a distinctive shelf-wide reflector, β2. Unit 3 shows an 'onlapping fill' reflection configuration over the highs developed by the underlying Unit 4 (Fig. 6). At the base of Unit 3 on the middle shelf, irregular erosional depressions along unconformity β3 are infilled, then the erosional surface is blanketed by gradually seaward-thinning, acoustically stratified deposits (Fig. 9A). Locally, the β3 surface is covered by numerous depositional mounds (Figs. 9B–E).

Unit 4 is divided into Subunits 4A and 4B. Subunit 4A underlies the erosional β3 unconformity in the area where progradational lobes have been mapped (Fig. 6), and forms a moderately reflective, onlapping deposit which progressively buried the relief of the underlying lobate mounds of Unit 5. Subunit 4B is only present toward the outer part of the shelf where it consists of a relatively thin prograded set of clinoforms that forms a narrow, flat-topped bench at present water depths of 55–60 m (Fig. 4). The β3 reflector can be traced into the landward feather-edge of the prograded deposit; hence, it is believed that Subunit 4B is coeval with the depositional break that formed β3 farther landward. Therefore Subunit 4B is inferred to be younger than Subunit 4A (Table 2).

Unit 5 is a south-prograded, lobate depositional sequence like Unit 2, but offset to the west of the younger sequence (Fig. 7B). The youngest clinoforms in Unit 5 are at a depth of approximately −69 m. Toward the outer part of the shelf, Unit 5 and the overlying Subunit 4A are generally missing or very thin because β3 and β4 merge with Q1 near the shelf edge (Figs. 4, 5 and 9A).

Based on the isopach maps of Fig. 7 and an acoustic velocity of 1500 m s^{-1}, the volumes of the lobate bodies forming Units 2 and 5 are, respectively, 0.39 km^3 and 0.33 km^3. Assuming an average porosity in these near-surface sediments of ∼40% (Hegarty et al., 1988) and a grain density of 2.65 g cm^{-3}, the masses of sediments in Units 2 and 5 are, respectively, 6.2×10^8 tonnes and 5.2×10^8 tonnes.

3.3. Interpretation of seismic units

The laterally continuous reflections in all the seismic units and the deep acoustic penetration suggest that the Quaternary succession is formed largely of interbedded silts and muds. Units 2 and 5 are interpreted as south-prograded delta lobes that developed on the northeastern Marmara Sea shelf. This is based on the lobate deposit shape (Fig. 7), and the clinoform geometry (Fig. 8). The clinoforms are inferred to be the foreset slopes of these deltas. They dip at angles $<3°$, consistent with a fine characteristic grain size (Hiscott, 2001). On the top of the Unit 2 delta, irregularly stratified, flat-lying deposits (Fig. 8) are interpreted as delta-top fluvial and wetland deposits. Toward the distal edges of the depositional lobes, Units 2 and 5 are interpreted to pass into prodeltaic silts and muds.

Units 1, 3 and 4A onlap underlying topography and fill depressions on the shelf. They resemble the distal prodeltaic muds of Units 2 and 5, but the youngest Unit 1 has formed since the establishment of two-layer flow in the Bosphorus (5.1. Chronology) when no deltas are known from the area of the strait. Hence, we interpret all of these

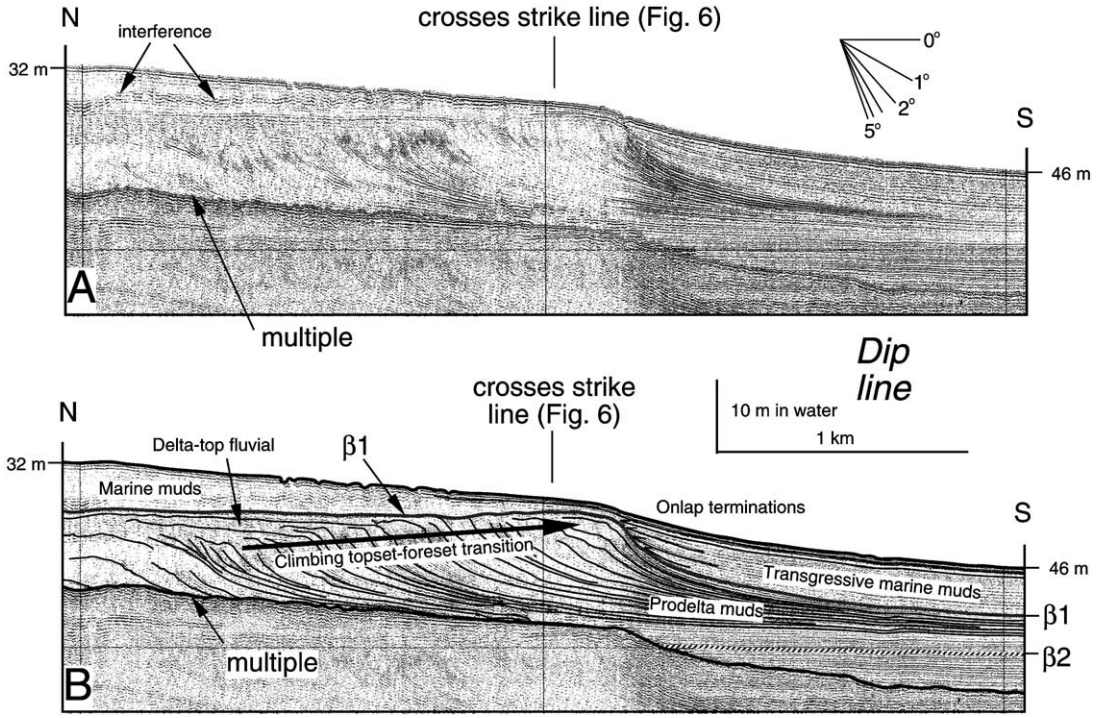

Fig. 8. Unmarked and interpreted Huntec DTS profile across clinoforms of Unit 2 (location in Fig. 3A). This seismic profile crosses the profile in Fig. 6, as indicated. The topset–foreset transition (offlap break) climbs consistently from north to south, indicating progradation during a relative sea-level rise (see text for discussion).

depression-filling, acoustically stratified deposits as marine muds and silts laid down on the shelf below storm wave base, with the sediment supplied by shelf currents, and possibly from the surface outflow from the strait. Holocene muds are widely distributed on the shelves of the Marmara Sea (Hiscott and Aksu, 2002), and likely have a multitude of sources including fringing small deltas of the southern shelf (e.g. Kocasu River, Fig. 1) and storm-induced advection of mud from inner-shelf areas. The depositional mounds that locally cover the β3 unconformity (Fig. 9B–E) are tentatively interpreted as algal–serpulid bioherms like those that have been sampled and dated from the crests of drowned sand bodies farther west in the Marmara Sea (Fig. 2; Aksu et al., 1999).

Locally crossbedded sediments in Subunit 4A (Fig. 10) are interpreted as sands reworked by shelf currents during the sea-level fall that formed the β3 unconformity (5.1. Chronology). The flat-topped bench formed by Subunit 4B on the outer shelf (Fig. 4) is interpreted, based entirely on its geometry and relationship to β3, as a beach/shoreline succession that formed seaward of the β3 exposure surface.

4. Core data

Three gravity cores constrain sedimentary facies, paleoceanography, and chronology of the latest Quaternary sediments above Q1: MAR97-11 (located on Fig. 1), MAR98-09 (Figs. 3 and 10), and MAR98-07 (Fig. 3). Table 1 lists core lengths, core site coordinates, water depths, and radiocarbon dates obtained for shells in each core.

4.1. Core MAR97-11

This core was raised from the southern shelf of the Marmara Sea (Fig. 1; Aksu et al., 1999, their fig. 12 at Fix 1684.1) and provides a record of

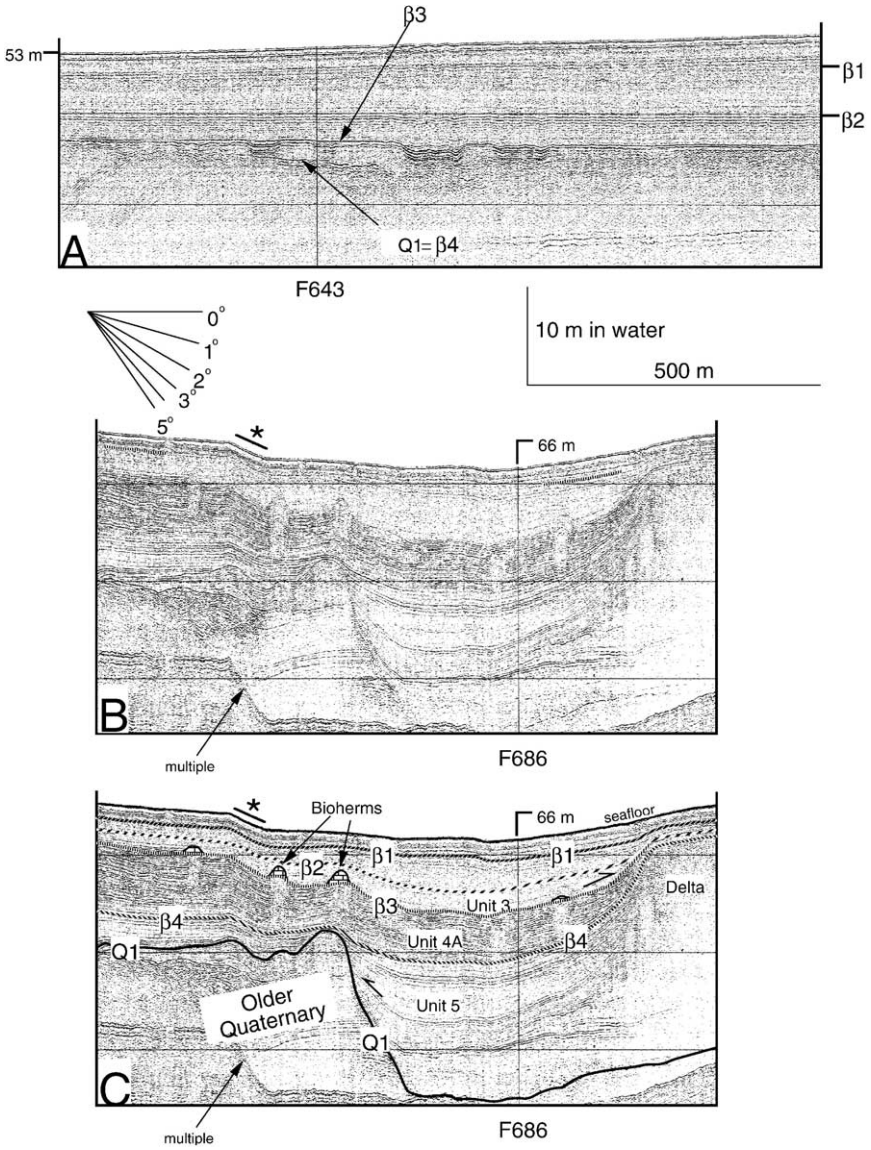

Fig. 9. Attributes of the β3 unconformity (locations in Fig. 3A). Bold bars beneath * signs mark places where raising or lowering of the Huntec towfish created apparent steps in the seafloor. (A) Erosional roughness along β3 on the outer shelf; in this area, β1 and β2 are conformable surfaces. (B and C) Unmarked and interpreted profile showing inferred bioherms along β3 adjacent to depositional highs of the Unit 5 delta. (D and E) Unmarked and interpreted profile showing exceptional development of inferred bioherms and erosional gulleys along the β3 unconformity.

paleoenvironmental conditions at the last lowstand (marine oxygen-isotopic stage 2) and during the marine invasion of the Marmara Sea after breaching of the Dardanelles Strait. The core was taken at a depth of 111 m in the toe-set of the most seaward lowstand delta of oxygen-isotopic stage 2, in a permanently subaqueous part of the basin. The basal part of the core (deeper than 65 cm) corresponds with southern shelf delta Δ2 of Aksu et al. (1999). The mud drape that has developed since this delta lobe was transgressed occupies 0–65 cm of the core and is younger

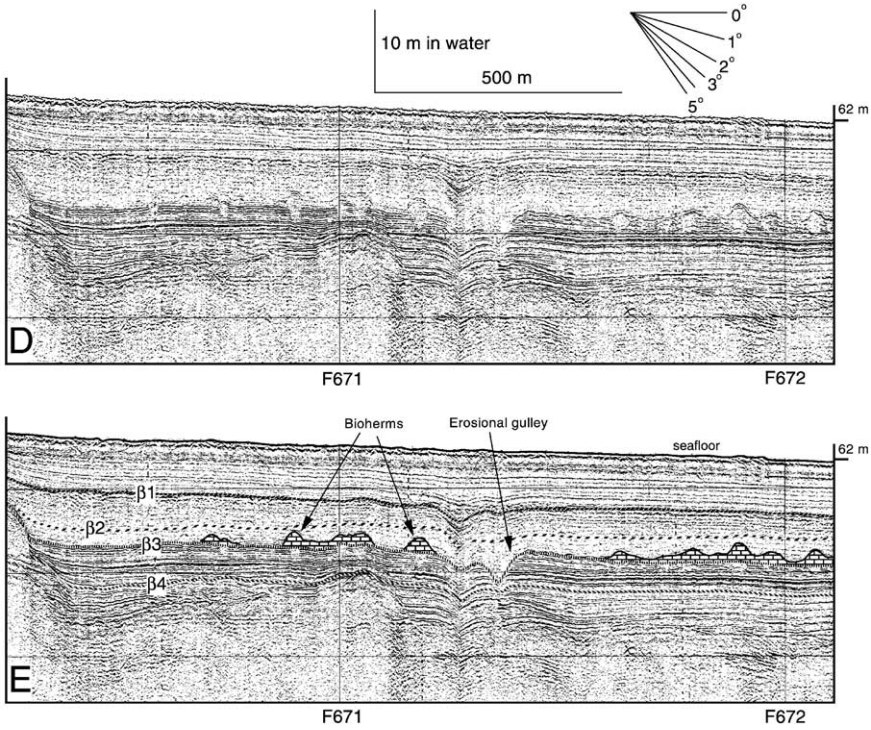

Fig. 9 (*Continued*).

than ~10.5 ka; on the western shelves of the Marmara Sea, this transgressive to highstand drape began to accumulate by ~11.5 ka, soon after reconnection with the Aegean Sea (Hiscott and Aksu, 2002).

Below a core depth of 100 cm (Fig. 11), the only mollusc present is *Dreissena rostriformis distincta*, a brackish- to fresh-water dweller, and foraminifera are absent except for rare specimens that could have been inmixed by burrowers or reworked from older strata. Dinoflagellate cysts (dinocysts) and other aquatic spores are predominantly (60–90%) brackish- to fresh-water taxa (Mudie et al., 2002a). These deposits accumulated when the southern shelf deltas were delivering abundant fresh-water to the near-shore zone, effectively excluding marine fauna and flora that continued to dwell in the central basins of the Marmara Sea (Aksu et al., 2002a).

Above a core depth of 100 cm, marine planktonic foraminifera (e.g. *Globigerina bulloides*, *G. quinqueloba*) and molluscs (e.g. *Varicorbula gibba*, *Turritella communis*, *Lucinoma borealis*) replace the non-marine fauna (Aksu et al., 2002a). The Marmara Sea was still isolated from the Aegean Sea at this time (~13 ka), so these marine fossils are not the remains of new immigrants from the Mediterranean, but rather represent a land-locked fauna that had survived in the Marmara Sea since its previous connection with the global ocean at ~22 ka (Aksu et al., 1999). At ~80 cm, marine benthic foraminifera become abundant (dominated by *Textularia*, *Cassidulina*, *Haynesina*, *Aubignyna* and *Fursenkoina*; Kaminski et al., 2002). *Fursenkoina acuta* and *Cassidulina carinata* both display typical behavior of 'pioneering' species in that they initially colonize the substrate in massive numbers owing to lack of competition from other marine species. Radiocarbon dates of 10 790 yr BP and 12 790 yr BP from 79–92 cm are consistent with drowning of the deltas when global sea level stood at −65 to −75 m (Fairbanks, 1989), just after breaching of the sill in the Dardanelles Strait. The sill was

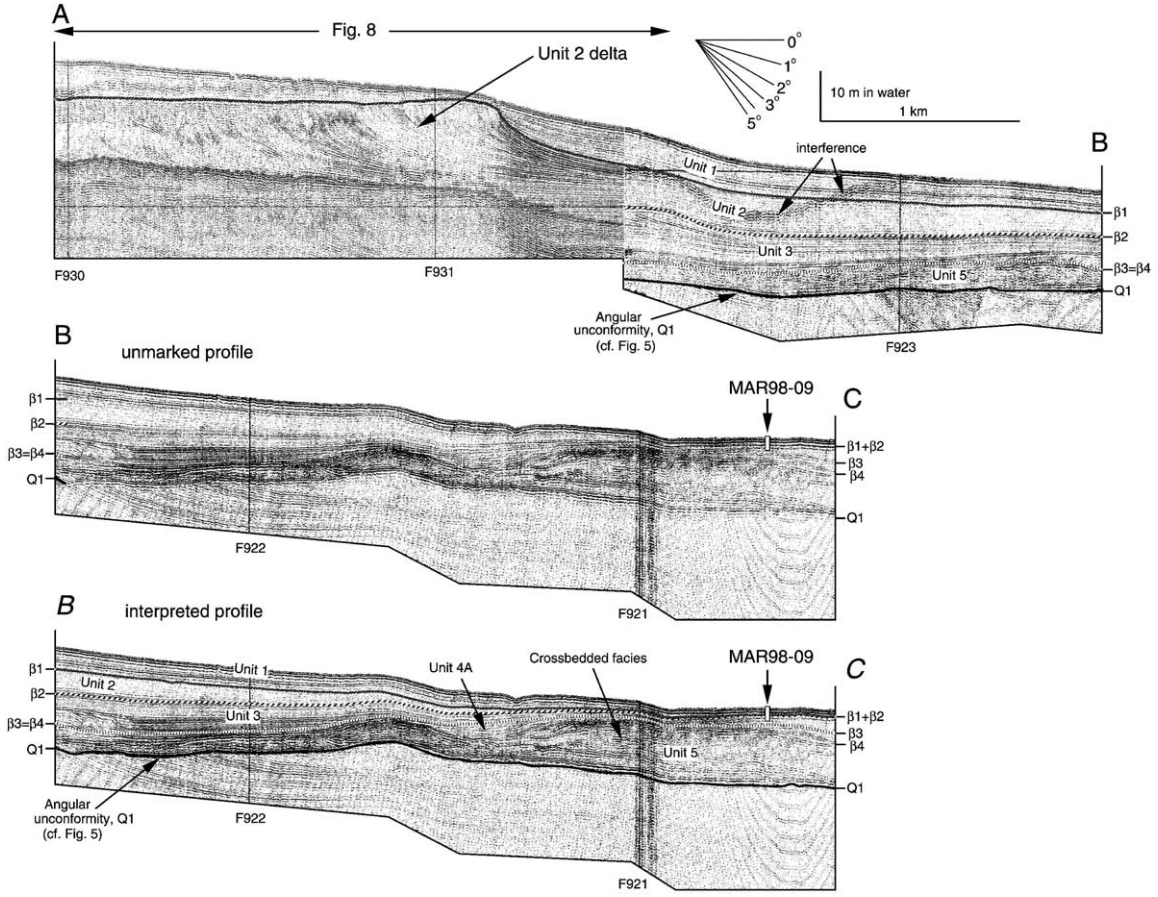

Fig. 10. Huntec DTS profile (A–B and B–C) that extends seaward from the Unit 2 progradational lobe (Fig. 8) to the MAR98-09 core site near the shelf edge, prepared by splicing together boomer records from adjacent tracks (profile locations in Fig. 3A). The entire latest Quaternary succession is shown (Units 1–5), lying unconformably above Q1. Panel A–B is also partly shown in Fig. 8, so no unmarked profile is presented. Panel B–C is provided as an unmarked (B–C) and interpreted (*B–C*) profile so that the reader can trace reflections to the core site.

about 5 m deeper at 12 ka than today (Yaltırak et al., 2002). The numbers of 'pioneering' benthic foraminifera decline upcore after the initial recolonization event, accompanied by diversification of the fauna (Kaminski et al., 2002). The percentages of the most marine species (*Brizalina* and *Bulimina*) fluctuate where total benthic concentrations are low, and then increase to dominate the benthic assemblage at a core depth of 75 cm (Fig. 11).

From 65 to 100 cm, the abundance of marine planktonic foraminifera and coccoliths is lower than nearer to the core top, and salinity estimates from foraminifera-based transfer functions (Aksu et al., 2002a) are 18–19‰. The salinity estimates rise to near-modern values of 21‰ above 60 cm. Coccoliths (e.g. *H. wallishii*, *H. selli*, *H. kemptaneri*, *Reticulofenestra* spp.) and Mediterranean dinocyst species (Mudie et al., 2002a) become common in the sediments above 90 cm (~12.0 ka). Total organic carbon (Abrajano et al., 2002) more than doubles to ~1.25% at a core depth of ~85 cm (~11.0 ka). The bloom of the infaunal benthic foraminifera *Fursenkoina* confirms an increase in carbon burial, as this genus is known to be an infaunal detritivore. The increasing coccolith abundances and TOC may signify the first, initially limited oceanographic connection of the

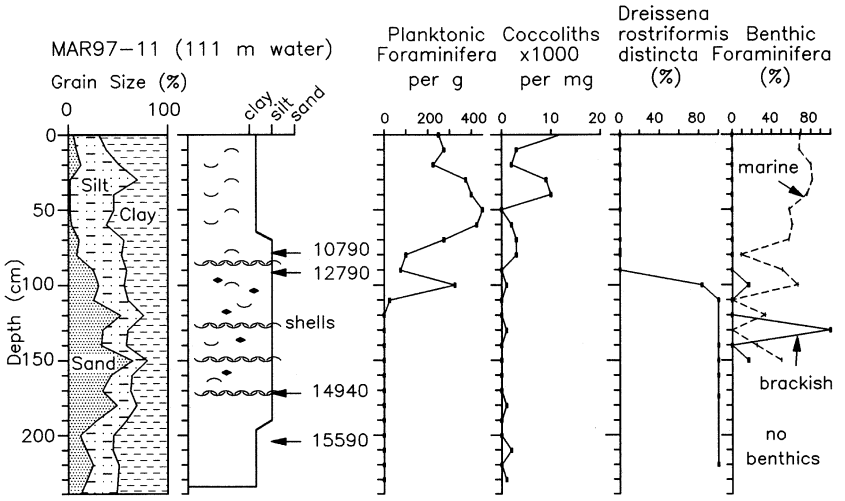

Fig. 11. Description of core MAR97-11 (Fig. 1) and downcore plots of paleontological data. In the benthic foraminifera column, the 'marine' percentage is the sum of *Brizalina* and *Bulimina* species; the 'brackish' percentage is the sum of *Ammonia* species. The core was taken at a water depth of 111 m. Details concerning radiocarbon dates are available in Table 1.

Marmara Sea to the Aegean Sea through the Dardanelles. The higher TOC is attributed to an increased stable stratification of the water column beneath what has become, since ~11.0 ka, a permanent fresher surface layer (Aksu et al., 2002a).

4.2. Core MAR98-09

Core MAR98-09 (Fig. 12) was collected from a water depth of 64 m on the outer shelf of the Marmara Sea south of the exit of the Bosphorus Strait (Fig. 3) where reflectors β1 and β2 converge. The seismically defined depth to β2 is ~125 cm (Fig. 10). The major lithologic boundaries in the core at 55 and 110 cm (Fig. 12) are interpreted to represent reflectors β1 and β2. Above β1 is the transgressive to highstand drape of Unit 1, characterized by uniformly high con-

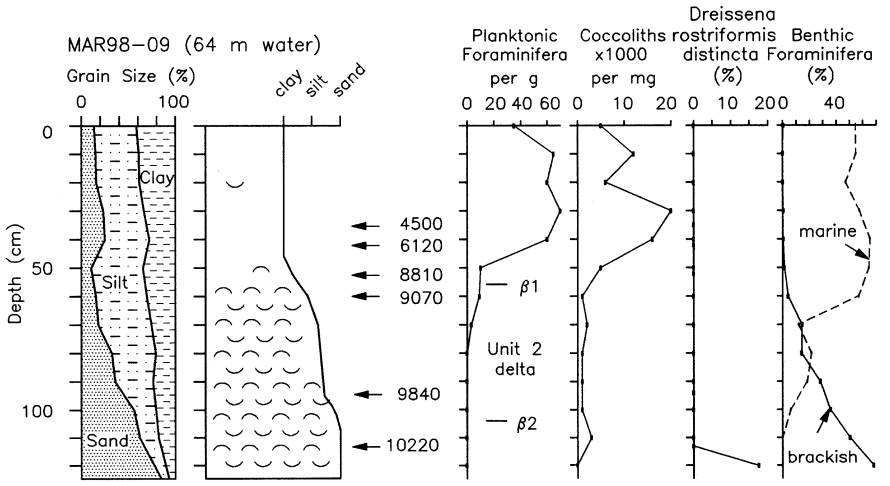

Fig. 12. Description of core MAR98-09 (Fig. 3A) and downcore plots of paleontological data. In the benthic foraminifera column, the 'marine' percentage is the sum of *Brizalina* and *Bulimina* species; the 'brackish' percentage is the sum of *Ammonia* species. The core was taken at a water depth of 64 m. Details concerning radiocarbon dates are available in Table 1.

tents of silt and clay. Radiocarbon dates (Table 1) constrain the ages of Units 1 and 2 to ~0–9.0 ka and ~9.0–10.0 ka, respectively. These proposed dates for Units 1 and 2 are corroborated in the next section of the paper by an independent method based on depths to topset–foreset transitions of the Unit 2 delta and the global sea-level curve of Fairbanks (1989), confirming the picks of β1 and β2 in the core (Fig. 12).

Marine molluscs are present throughout the core, but are most abundant below a core depth of 35 cm. The most abundant species are *Turritella communis*, *Varicorbula gibba*, *Ceratoderma glaucum*, and *Nucula nucleus* (MacDonald, 2000). Ostracods are present throughout the core in relatively small numbers and document a transition from non-marine (but probably not fresh-water) to marine conditions. The great majority of specimens are juveniles, which limits their identification to the genus level. The older samples (below 60 cm) contain the genera *Loxoconcha*, *Leptocythere* and *Cyprideis*. *Loxoconcha* and *Leptocythere* prefer very shallow-marine conditions and salinities of ~20–30‰ (Athersuch et al., 1989). Samples collected higher in the core (0–10 cm) contain mostly *Charinocythereis*, which is a deeper marine form that prefers a salinity of about 30‰.

Benthic foraminiferal and dinocyst assemblages in the core reflect a history of increasing paleowater depth through time, as the site became increasingly marine. The foraminifera at the base of the core (100–120 cm) are abundant, but display a low diversity and are completely dominated by *Ammonia* with only rare specimens of *Textularia* and *Elphidium*. This impoverished assemblage reflects shallow-water conditions and lowered salinity. Dinocyst assemblages have ~30% fresh-water species (Mudie et al., 2002a). From 100 to 50 cm (younger than ~10 ka; Table 1), benthic foraminifera are more diverse, with increasing numbers of *Nonionella*, *Bulimina*, *Brizalina*, *Fursenkoina* and *Lobatula*. This faunal change reflects increasing water depths and the presence of a more stratified water column. The appearance of infaunal forms indicates reduced oxygen content beneath the surface mixed layer of the water column. Above 40 cm, *Ammonia* disappears from the record, and the assemblage is dominated by *Brizalina* and *Bulimina*, indicating deposition beneath a permanently stratified water column (Fig. 12). The dinocyst and other algal spore assemblages above ~50 cm core depth show a reduction in fresh-water taxa and an increase in hypersaline Mediterranean taxa.

Surface-dwelling planktonic foraminifera (mainly *G. quinqueloba* with minor *Globigerina bulloides*, *Neogloboquadrina pachyderma*, *G. ruber*, *G. uvula*) and coccoliths (mainly *Emiliania huxleyi*, *Reticulofenestra* spp.) are essentially absent below a core depth of 50 cm (~8.8 ka; Table 1), downward from which only reworked coccoliths occur (Aksu et al., 2002a). Benthic foraminifera are identical to modern types above ~60 cm core depth, but include abundant brackish-water species *A. beccarii* and *A. inflata* below that depth (Kaminski et al., 2002). The sharp decline in planktonic microfossils at 50 cm depth probably reflects dilution by terrigenous sediment, because the uncorrected sedimentation rate is 34 cm/kyr below this level but only 3.6 cm/kyr at shallow depths (based on age–depth plot from Table 1).

4.3. Core MAR98-07

Core MAR98-07 (Fig. 13) was raised near the shelf edge in 95 m of water. During the last glacial lowstand of oxygen-isotopic stage 2, the water level in the Marmara Sea stood at about −100 to −90 m (Aksu et al., 1999; Smith et al., 1995), so this core site would have been near the paleoshoreline of the stage 2 Marmara Sea lake. The lower part of the core, below 70 cm, contains only fresh-water fauna, predominantly the fresh- to brackish-water mollusc *Dreissena rostiformis distincta* (MacDonald, 2000). Benthic foraminifera occur sporadically below 70 cm, and are present to the base of the core. The occurrence of species such as *Haynesina depressula*, *Aubignyna perlucida* and *Ammonia compacta*, which are rare in the overlying marine unit, indicates reworking from older Quaternary marine sediments (Kaminski et al., 2002). The deeper part of the core penetrated deposits below unconformity Q1, older than ~40 ka (Table 1). The Q1 unconformity, placed at ~80 cm depth, is coincident at

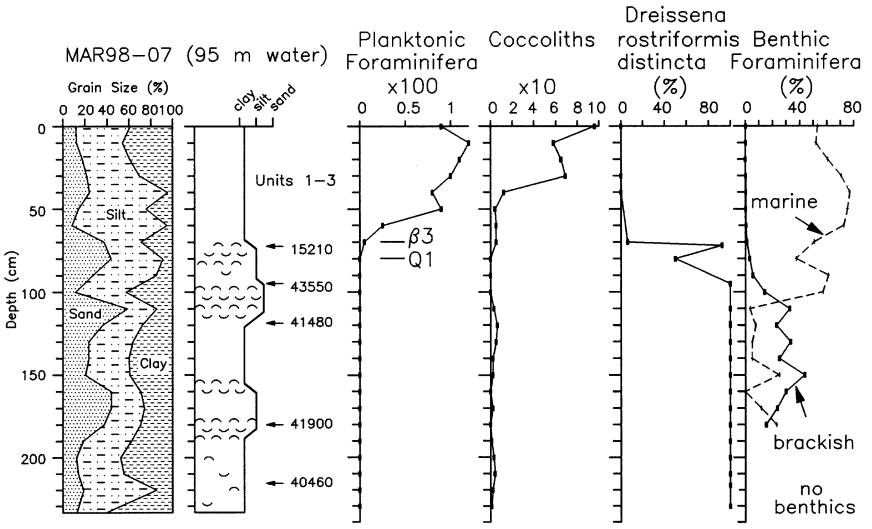

Fig. 13. Description of core MAR98-07 (Fig. 3A) and downcore plots of paleontological data. In the benthic foraminifera column, the 'marine' percentage is the sum of *Brizalina* and *Bulimina* species; the 'brackish' percentage is the sum of *Ammonia* species. The core was taken at a water depth of 95 m. Details concerning radiocarbon dates are available in Table 1.

this site with surfaces β3 and β4 because of reflector convergence near the shelf edge. Based on a date of 15 210 yr BP (Table 1), 80–70 cm is assigned to Subunit 4B (Table 2) whereas 70–0 cm is correlated with seismic Units 1–3.

Above core depths of 70 cm, marine molluscs become common (*Varicorbula gibba*, *Ceratoderma glaucum*, *Apporhais pespelecani*, *Lucinoma borealis*; MacDonald, 2000), as do planktonic foraminifera (mainly *G. quinqueloba*) and coccoliths (mainly *H.* spp. and *Emiliania huxleyi*). Planktonic foraminifera and coccoliths are particularly common above 50 cm (Fig. 13). Benthic foraminifera show an abrupt increase in numbers and diversity at 70 cm. The assemblage recovered from 70–60 cm is dominated by *Bulimina*, *Brizalina* (Fig. 13), *Cassidulina* and *Nonionella*, indicating that normal marine conditions were established rapidly after β3 time. No shallow-water *Ammonia*-dominated assemblage was found at the base of this marine interval. Higher in the core (above 50 cm), the proportions of *Cassidulina* and *Nonionella* decrease, and *Bulimina*, *Polymorphina*, *Biloculinella* and *Hyalina* increase, reflecting deeper marine conditions in a stratified water column (Kaminski et al., 2002).

The lack of an *Ammonia*-dominated benthic foraminiferal assemblage immediately above β3 suggests rapid drowning during the Holocene transgression. Aksu et al. (1999) noted that the deepest topset–foreset transition of lowstand deltas along the southern shelf of the Marmara Sea is at a modern water depth of ~100 m (see also Smith et al., 1995), implying a stage 2 lowstand of perhaps −90 to −95 m. The rapid drowning observed in core MAR98-07 may have occurred when rising waters of the Aegean Sea overtopped the sill in the Dardanelles Strait at ~12 ka, causing water levels in the small Marmara Sea basin to rise rapidly from −95 m to −75 m. This drowning would have triggered a sharp increase in salinity and the onset of widespread mud deposition. High-resolution seismic profiles presented by Aksu et al. (1999) show that hemipelagic muds overlie the lowstand unconformity with no intervening reworked veneer where water depths exceed ~80 m in the western Marmara Sea. This observation supports the hypothesis of a drowning so rapid (perhaps lasting only a few tens of years) that reworking was unable to leave an imprint.

5. Age and significance of the deltas of Units 2 and 5

5.1. Chronology

In core MAR98-07, the sediments below Q1 are older than ~40 ka (Table 1). The ~40-ka dates must be viewed with caution, however, because subaerial exposure might have leached these shells and made them susceptible to later contamination with younger carbon following the Holocene transgression (e.g. Yim, 1999). The shells in this interval are, in fact, chalky in appearance. If contamination by young carbon took place, then the shells could actually be older than 50 ka (the lower limit for radiocarbon dating) and of indeterminate age. There are strong arguments in favor of a >50-ka age. The chalky shells are non-marine (possibly estuarine) species, yet from ~25 to 125 ka (oxygen-isotopic stages 3–5) the water depth at this site was consistently greater than ~45 m (Fig. 14). Not until glacial oxygen-isotopic stage 6, ending at ~125 ka, was global sea level drawn down to just below the depth of the bedrock sill in the Dardanelles Strait. This sill was then at an elevation of ~−105 m, considerably deeper than today because of subsequent persistent uplift of 0.40 mm/yr (Yaltırak et al., 2002). Such a profound lowstand would have subaerially exposed the entire shelf, forming Q1. Based on the sea-level curve of Skene et al. (1998; Fig. 14), we propose that the lower part of core MAR98-07 is older than the initiation of this lowstand at ~160 ka (Table 2), and that the radiocarbon dates of 42–40 ka have resulted from contamination of leached shells by young carbon.

When the MAR98-07 core site was transgressed by global sea-level rise shortly after 125 ka (Fig. 14), accommodation space would have become available for the deposition of Units 5 and 4. However, the sediment volume in the Unit 5 delta (0.33 km^3) and its location immediately south of the exit of the strait (Fig. 7B) have convinced us that this delta could have formed only when the Black Sea was spilling southward through the Bosphorus Strait. Indeed, there are no local rivers of sufficient size to have supplied the sediment present in this delta or for that matter in the Unit 2 delta (see calculation in 5.2. Development of the Unit 2 delta).

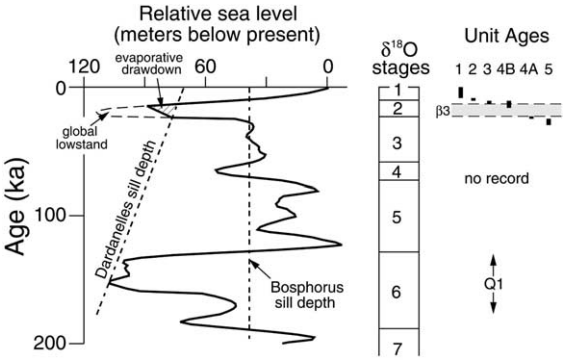

Fig. 14. Sea-level curve of Skene et al. (1998), modified at lowstands to recognize that the Marmara Sea initially fell no lower than the sill depth in the Dardanelles Strait – subsequent evaporation at the lowstand is believed to have further depressed water levels by ~20 m at 13 ka, just before breaching of the strait by the rising global ocean. Sea-level variation is shown back to ~200 ka, when the floor of the Dardanelles was much deeper than at present because of persistent tectonic uplift since that time (Yaltırak et al., 2002). Age estimates for Units 1–5, β3 and Q1 are explained in the text.

When since ~125 ka did the Black Sea spill into the Marmara Sea through the Bosphorus Strait? Aksu et al. (2002b) record a step-wise transgression of the southern Black Sea shelf that began from a shoreline elevation of ~−100 m at ~10.5 ka or earlier. By no later than ~10–9.5 ka, the Black Sea rose to the sill depth of the Bosphorus Strait (~−40 m) and started to overspill into the Marmara Sea. The transgression on the southern Black Sea shelf may have commenced earlier than 10.5 ka, perhaps as early as ~13 ka (Aksu et al., 2002b). This would have permitted Black Sea overflow to begin as early as perhaps 10.6 ka when a widespread sapropel layer began to be deposited in basins of the Marmara Sea (Çağatay et al., 2000). Radiocarbon ages in core MAR98-09 (Fig. 12) and the thickness of sediments between the base of this core and Q1 (Fig. 10) rule out any possibility that the Unit 5 delta could have formed after the Black Sea began to spill over into the Marmara Sea at ~10.5–10 ka. There is simply too much sediment to have accumulated in only a few hun-

dred years. There is also a significant hiatus above the Unit 5 delta and Subunit 4A, at the β3 unconformity, when sea level appears to have fallen to at least −55 to −60 m (Subunit 4B bench). We propose that the prominent β3 unconformity developed by subaerial exposure of Subunit 4A and Unit 5 during the relatively short lowstand of oxygen-isotopic stage 2 (~22–12 ka; Fig. 14) because this is the only time after stage 6 when the inner to middle shelf was subaerially exposed. Subunit 4B is interpreted to partly overlap in age with development of the β3 unconformity (Table 2), so that the shell dated at 15.2 ka in core MAR98-07 is provisionally assigned to this subunit.

Units 5 and 4A, therefore, have a poorly constrained age of 125–22 ka (oxygen-isotopic stages 5–3). The Bosphorus Strait is believed to be younger than ~100 ka (Oktay et al., 2002). Prior to its opening, another strait situated farther to the east near the mouth of the present-day Sakarya River connected the Black Sea to the Marmara Sea (Pfannenstiel, 1944). Hence, the Unit 5 delta can be no older than ~100 ka. The elevation of the youngest foresets of the Unit 5 delta suggests a contemporary sea level of −57 m, assuming no post-depositional subsidence. Such moderately depressed water levels are characteristic of oxygen-isotopic stage 3 (59–22 ka) when the Marmara Sea maintained a connection with the Aegean Sea through the Dardanelles (Fig. 14; Aksu et al., 1999). Mediterranean sapropel S2 has an age in the range 60–40 ka, and may have formed at the same time as Unit 5, when an earlier pulse of relatively fresh-water was discharged from the Black Sea through the Bosphorus Strait. Alternatively, the deposition of the Unit 5 delta might coincide with the accumulation of Marmara Sea sapropel M2 at ~29.5–23.5 ka (Aksu et al., 2002a). According to Görür et al. (2001), the sedimentary infill of the Bosphorus Channel indicates that the Black Sea spilled into the Marmara Sea from 30 to 22 ka, during the same time that sapropel M2 was accumulating. We therefore prefer an age within oxygen-isotopic stage 3 for the accumulation of this delta and the overlying Subunit 4A (Table 2).

Unit 3 includes the first deposits of the Holocene transgression above lowstand unconformity β3, and hence should be no older than ~12 ka when the Dardanelles was first breached and Mediterranean waters flooded the Marmara Sea shelves. Radiocarbon dates in core MAR98-09 suggest that the Unit 2 delta (Fig. 10) accumulated from ~10 to 9 ka, bracketing Unit 3 to ~12–10 ka. Unit 1 has accumulated since ~9 ka during a time when a significant salt wedge and then two-layer flow became established in the Bosphorus Channel, cutting off the supply of bedload to the Unit 2 delta.

5.2. Development of the Unit 2 delta

Fresh surface-water outflow in the Unit 2 prodelta area is demonstrated by micropaleontological data for core MAR98-09 (Fig. 12). Although there are persistent marine bottom-dwelling molluscs and benthic foraminifera older than ~10 ka, marine microplankton are absent until ~9 ka. Only benthic foraminifera tolerant of low salinities (*Ammonia*) are present. This suggests that the surface outflow from delta distributaries was sufficiently fresh and vigorous to exclude open-marine surface dwellers.

The delta is restricted to the inner shelf with a topset–foreset transition at ~40 m water depth, so apparently was not active when the level of the Marmara Sea was at its lowest (~−90 m at ~12 ka; Aksu et al., 1999). Modern topset–foreset transitions in the wave-influenced Marmara Sea are at water depths of ~10 m (Aksu et al., 1999), so the delta likely formed when sea level was ~30 m below present. Global and Mediterranean sea level reached this height at ~9.0 ka, based on the Barbados sea-level curve (Fairbanks, 1989). This is in remarkable agreement with radiocarbon dates for the delta (Fig. 12). Also at ~9 ka, *Ammonia* declines in abundance and the first planktonic foraminifera and coccoliths are found in post-deltaic sediments, indicating that fresh-water outflow from the strait had declined to the point that more stenohaline species could establish themselves. Shortly before 9 ka, benthic foraminifera of Mediterranean origin colonized the prodelta fringe, suggesting that a salt wedge or estuarine-type flow had been established during

the latter phases of delta advance (Kaminski et al., 2002).

Kukal (1971, p. 38) indicates that ~60% of the sediment carried by a mixed-load river is used to construct its delta, whereas the remainder is carried farther offshore to contribute to shelf and basinal mud deposits. If this ratio is appropriate to the Unit 2 delta, then the total sediment yield in ~1000 yr would have been $(6.2\times10^8$ tonnes)/$0.6 = 1.03\times10^9$ tonnes, or 1.03×10^6 tonnes yr^{-1}. This is about half the sediment discharge of the Kocasu River (Fig. 1), which is the biggest modern river entering the southern shelf of the Marmara Sea (Aksu et al., 1999). A river of this size should have been able to construct a prominent lowstand delta when the level of the Marmara Sea was ~−90 m, yet no delta is present at these depths on the shelf south of the Bosphorus Strait. We conclude that Black Sea outflow was either weak at this time (~12 ka) or had not yet begun. A comparison with the sediment discharge of the modern Kocasu River is useful because it emphasizes the enormous mismatch between the scale of the Unit 2 delta and that of the small creeks that currently drain onto the shelf of the northern Marmara Sea near Istanbul.

Lowstand deltas of the southern Marmara Sea shelf, like the Kocasu River delta, were quickly driven landward during the Holocene transgression (Aksu et al., 1999). This was the normal behavior of most marine deltas during the Holocene – they were unable to continue to prograde except when the rate of relative sea-level rise was slow, and instead suffered rapid transgression and backstepping. In contrast, the Unit 2 delta shows a remarkable phase of seaward progradation when the topset–foreset transition climbed upward from −46 m to −40 m (Fig. 8). Assuming little or no compactional subsidence, this progradation occurred as global sea level rose from −36 m to −30 m, corresponding to dates of 9.3–9.0 ka (Fairbanks, 1989). The only way that a small marine delta can aggressively prograde ~2 km in 300 yr into a regionally transgressing ocean is if the short-term rate of sediment supply is very high.

What was the source of the suspended load and bedload for construction of the Unit 2 delta? This is a non-trivial question, because the Bosphorus Strait has no headwaters from which to derive detritus. Instead, sediment must have been excavated from the floor of the strait itself. It may not be coincidence that the progradation of this delta ceased when sea level had reached ~−30 m. As sea level continued to rise even higher, the southern end of the Bosphorus 'river' would have first become inundated, and then a two-way flow would have started to develop in the strait, so that the less dense Black Sea outflow would have been separated from the seabed by an intruding wedge of saline Mediterranean water. When this happened, the south-moving outflow would have been transformed into a clear-water surface current, and delta growth would have ceased. In line with this prediction, the persistence of sapropel deposition in the Aegean Sea until ~6.4 ka suggests that vigorous brackish-water outflow from the Black Sea did not diminish until well after delta growth ceased, and long after the development of two-layer flow in the Bosphorus. The imprint of the low-salinity discharge at core site MAR98-09 became less after ~9 ka only because the exit of the strait shifted considerably landward, allowing sufficient incursion of marine surface waters so that planktonic foraminifera and coccoliths could accumulate in bottom sediments.

Once spillover into the Marmara Sea began, delta lobes developed at the exit of the strait, west-directed bedforms formed in the western Marmara Sea (Aksu et al., 1999), and stratification of the water column in both the Marmara Sea and Aegean Sea led to accumulation of organic-rich sapropel deposits beginning at ~10.6 ka (Çağatay et al., 2000).

5.3. Relevance to late Quaternary history of the Marmara and Black seas

The chronology derived from seismic and core studies south of the Bosphorus Strait (Table 2) can be readily integrated with other paleoceanographic events derived from our ongoing research (Fig. 15). The geological history recorded in Fig. 15 is entirely incompatible with the suggestion by Ryan et al. (1997) that there was no connection

between the Black Sea and Marmara Sea until ~7.15 ka, and that the connection involved northward flow of Mediterranean water into the Black Sea. We instead propose that the Black Sea rose from a late Pleistocene low of ~−120 m to the Bosphorus sill depth by ~10–10.5 ka, and then started a long-term net outflow into the eastern Mediterranean Sea via the Marmara Sea that continues to the present day, with a particularly strong pulse at ~10.0–9.0 ka (Unit 2 delta). All evidence points to a persistently stratified water column in the Marmara Sea since at least 10.5 ka (e.g. high TOC and pollen–spore concentrations reported by Abrajano et al. (2002), dominance of benthic foraminifera *Brizalina* and *Bulimina* as reported by Kaminski et al. (2002), early Holocene dominance of brackish- to fresh-water dinocysts reported by Mudie et al. (2002a), onset of sapropel deposition at ~10.6 ka reported by Çağatay et al. (2000) and Aksu et al. (2002a)). If there had been a catastrophic flooding of the Black Sea at ~7.15 ka as proposed by Ryan et al. (1997), then stratification would have been impossible, as the rapid inflow of Aegean Sea water into (and across) the Marmara Sea would have disrupted the estuarine-type circulation of the Marmara Sea and guaranteed a well-mixed and well-oxygenated water column. Instead, core data provide no evidence whatsoever for an influx of Mediterranean species at ~7.15 ka, and benthic foraminiferal assemblages demonstrate that the Marmara Sea experienced reduced oxygenation beneath a persistent halocline since ~11 ka without any return to well-oxygenated conditions. Furthermore, pollen data for Black Sea cores show no evidence for agricultural settlement before ~4 ka or for catastrophic inundation of shoreline vegetation during the Holocene (Mudie et al., 2002b).

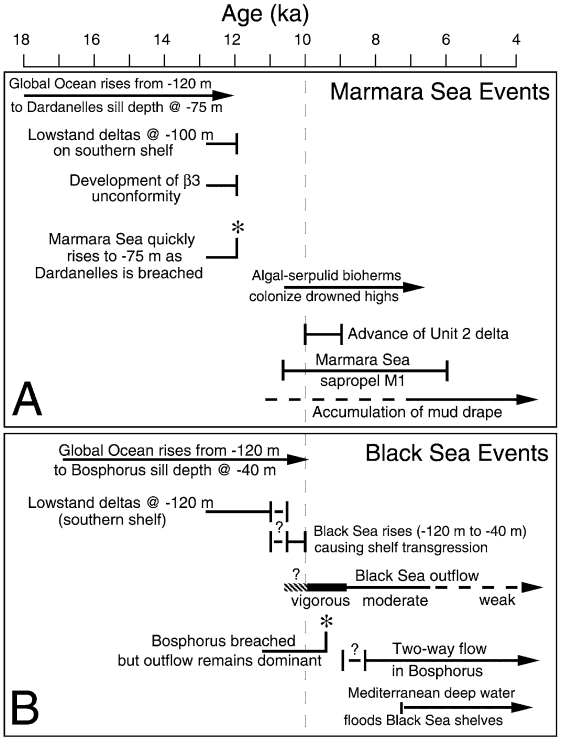

Fig. 15. Summary of the paleoceanographic history of the region south (A) and north (B) of the Bosphorus Strait, consistent with the findings of this paper and with those of Aksu et al. (2002b) for the Black Sea shelf north of the Bosphorus Strait.

We stand by the arguments that Aksu et al. (1999) used to explain the young ages of postglacial pioneering marine bivalves collected from the northern Black Sea shelves by Ryan et al. (1997). These ~7.15-ka shells do not, in our view, date the first connection of the Marmara Sea and the Black Sea at ~10 ka, but instead lag this first connection by more than 2000 yr, during which time a two-way flow became established in the Bosphorus Strait (Fig. 15, Lane-Serff et al., 1997). Slowly, denser, more saline Mediterranean water filled the Black Sea basin by displacing a lower salinity surface layer. Open-marine fauna could successfully colonize the Black Sea shelves only when the surface layer had thinned to less than ~150 m. In contrast, the Marmara Sea, because of its much smaller size, underwent a rapid change to marine conditions once the Dardanelles Strait was breached at ~12 ka, perhaps involving a rapid flooding of the Marmara Sea basin to raise its water level from −95 m to −75 m in a short time period (see 4.3. Core MAR98-07). The Dardanelles Strait is significantly wider than the Bosphorus Strait, so a free connection between the Mediterranean and Marmara seas would have been easier to establish in a short interval of time.

6. Conclusions

Short periods of vigorous south-directed outflow from the Black Sea, through the Bosphorus Strait, were responsible for the transport of sediments onto the northeastern Marmara shelf, and their deposition in the lobate deltas of Units 2 and 5. Because the topset–foreset transition in active deltas in the region occurs at ~10 m water depth, the Unit 2 delta is inferred to have ceased its progradation when sea level stood at −30 m, approximately equal to the minimum depth of the Bosphorus Strait at −40 m. The southward climb of the topset–foreset transition (Fig. 8) indicates that delta progradation took place during a period of water-level rise in the Marmara Sea, when sediment supply was sufficiently high to allow progradation as well as vertical accretion.

The absence of north-prograded deposits on the southwestern Black Sea shelf north of the Bosphorus (Aksu et al., 2002b) and the presence of south-prograded stacked deltas on the northeastern Marmara Sea shelf south of the Bosphorus (Figs. 6–8 and 10) are entirely inconsistent with the suggestion of Ryan et al. (1997) that the Black Sea was re-filled during the Holocene by a rapid influx of Mediterranean water via the Bosphorus. Instead, a variety of sedimentological and paleontological data strongly support the view of Aksu et al. (1999) that the Black Sea flowed southwestward into the Aegean Sea through the Marmara Sea subsequent to the deglaciation of Europe, as the climate became more humid and rivers entering the Black Sea increased their discharges. Major rivers like the Danube, Dniester, Dnieper, Southern Bug and Don Rivers gradually filled the Black Sea basin, forming a transgressive systems tract on the southern Black Sea shelf (e.g. backstepping barrier islands; Aksu et al., 2002b). Then, at ~10 ka or perhaps as early as 10.6 ka, the rising Black Sea spilled through the Bosphorus Strait into the Marmara Sea, constructed the Unit 2 delta at the southern end of the strait, developed a vigorous southward flow toward the Aegean Sea, formed west-directed bedforms in the western Marmara Sea, and initiated deposition of sapropel S1 in the Aegean Sea by ~9.5 ka after a sufficiently thick surface layer of low-salinity water had developed there, and sapropel M1 in the Marmara Sea by ~10.6 ka. When outflow weakened at ~6.5 ka, sapropel deposition ceased in the Aegean Sea and a transgressive to high-stand mud drape continued to accumulate in the Marmara Sea. Since at least 10.5–11 ka, the Marmara Sea has been characterized by an estuarine-type circulation that has promoted stratification of the water column, elevated TOC concentrations in bottom sediments, and diagnostic benthic foraminiferal communities of infaunal detritivores. This circulation depends entirely on a persistent outflow of low-salinity water from the Black Sea, providing today about 50 times the discharge of all the rivers that enter the Marmara Sea.

Two delta lobes have been deposited at the southern end of the Bosphorus Strait by pulses of brackish-water outflow from the Black Sea. The most recent accumulated during ~10–9 ka, and an older lobe is inferred to have accumulated during oxygen-isotopic stage 3, most likely from ~29.5 to 23.5 ka, when sapropel M2 was deposited in the Marmara Sea.

Acknowledgements

We thank Prof. Dr. Erol Izdar, the Director of the Piri Reis Foundation for Maritime and Marine Resources Development and Education, and Prof. Dr. Orhan Uslu, the Director of the Institute of Marine Sciences and Technology, for their support and encouragement. We extend our special thanks to the officers and crew of the RV *Koca Piri Reis* for their assistance in data acquisition, in particular Captains Mehmet Özsaygılı (MAR98) and Ramiz Akdemir (MAR00) and the Chief Engineer Ömer Çubuk. We acknowledge research and ship-time funds from the Natural Sciences and Engineering Research Council of Canada (NSERC) to A.E.A. and R.N.H., travel funds from the Dean of Science, Memorial University of Newfoundland, and a special grant from the Piri Reis Foundation for Maritime and Marine Resources Development and Education.

References

Abbott, R.T., Dance, S.P., 1998. Compendium of Seashells. Odysey Publ., El Cajon, CA, 411 pp.

Abrajano, T., Aksu, A.E., Hiscott, R.N., Mudie, P.J., 2002. Aspect of carbon isotope biogeochemistry of late Quaternary sediments from the Marmara and Black Seas. Mar. Geol. 190, S0025-3227(02)00346-8.

Aksu, A.E., Yaşar, D., Mudie, P.J., 1995a. Paleoclimatic and paleoceanographic conditions leading to development of sapropel layer S1 in the Aegean Sea basins. Palaeoclimatol. Palaeogeogr. Palaeoecol. 116, 71–101.

Aksu, A.E., Yaşar, D., Mudie, P.J., Gillespie, H., 1995b. Late glacial–Holocene paleoclimatic and paleoceanographic evolution of the Aegean Sea: micropaleontological and stable isotopic evidence. Mar. Micropaleol. 25, 1–28.

Aksu, A.E., Hiscott, R.N., Yaşar, D., 1999. Oscillating Quaternary water levels of the Marmara Sea and vigorous outflow into the Aegean Sea from the Marmara Sea–Black Sea drainage corridor. Mar. Geol. 153, 275–302.

Aksu, A.E., Calon, T.J., Hiscott, R.N., Yaşar, D., 2000. Anatomy of the North Anatolian Fault Zone in the Marmara Sea, western Turkey: extensional basins above a continental transform. GSA Today 10 (6), 3–7.

Aksu, A.E., Hiscott, R.N., Kaminski, M.A., Mudie, P.J., Gillespie, H., Abrajano, T., Yaşar, D., 2002a. Last glacial–Holocene paleoceanography of the Black Sea and Marmara Sea: stable isotopic, foraminiferal and coccolith evidence. Mar. Geol. 190, S0025-3227(02)00345-6.

Aksu, A.E., Hiscott, R.N., Yaşar, D., Işler, F.I., Marsh, S., 2002b. Seismic stratigraphy of Late Quaternary deposits from the southwestern Black Sea shelf: evidence for non-catastrophic variations in sea-level during the last 10 000 years. Mar. Geol. 190, S0025-3227(02)00343-2.

Athersuch, J., Horne, D.J., Whittaker, J.E., 1989. Marine and Brackish Water Ostracods (Superfamilies Cypridacea and Cytheracea). Synopses of the British Fauna, No. 43. E.J. Brill, Leiden, 343 pp.

Beşiktepe, Ş, Sur, H.I., Özsoy, E., Latif, M.A., Oğuz, T., Ünlüata, Ü., 1994. The circulation and hydrography of the Marmara Sea. Prog. Oceanogr. 34, 285–334.

Bogdanova, C., 1969. Seasonal fluctuations in the inflow and the distribution of the Mediterranean waters in the Black Sea. In: Fomin, L.M. (Ed.), Basic Features of the Geological Structure, the Hydrological Regime and Biology of the Mediterranean Sea. Academy of Science, Moscow. English translation by Institute of Modern Languages, Washington, DC, pp. 131–139.

Brown, D., 1999. 'Great Flood' Theory passes science test: Dam! Where did all that water come from. AAPG Explorer, April 1999, pp. 47–67.

Çağatay, M.N., Görür, N., Algan, O., Eastoe, C., Tchepalyga, A., Ongan, D., Kuhn, T., Kuşcu, I., 2000. Late Glacial–Holocene palaeoceanography of the Sea of Marmara: timing of connections with the Mediterranean and the Black Seas. Mar. Geol. 167, 191–206.

Emeis, K., Shipboard Scientific Party, 1996. Paleoceanography and sapropel introduction. Proc. ODP Init. Reports 160, 21–28.

Fairbanks, R.G., 1989. A 17 000-year glacio–eustatic sea level record: influence of glacial melting rates on the Younger Dryas event and deep-ocean circulation. Nature 342, 637–642.

Görür, N., Çağatay, M.N., Emre, Ö., Alpar, B., Sakınç, M., Islamoğlu, Y., Algan, O., Erkal, T., Keçer, M., Akkök, R., Karlık, G., 2001. Is the abrupt drowning of the Black Sea shelf at 7150 yr BP a myth? Mar. Geol. 176, 65–73.

Hegarty, K.A., Weisel, J.K., Mutter, J.C., 1988. Subsidence history of Australia's southern margin: constraints on basin models. Am. Assoc. Petrol. Geol. Bull. 72, 615–633.

Hiscott, R.N., 2001. Depositional sequences controlled by high rates of sediment supply, sea-level variations, and growth faulting: the Quaternary Baram Delta of northwestern Borneo. Mar. Geol. 175, 67–102.

Hiscott, R.N., Aksu, A.E., 2002. Late Quaternary history of the Marmara Sea and Black Sea from high-resolution seismic and gravity core studies. Mar. Geol. 190, S0025-3227(02)00350-X.

Kaminski, M.A., Aksu, A.E., Hiscott, R.N., Box, M., Al-Salameen M., Filipescu, S., 2002. Late glacial to Holocene benthic foraminifera in the Marmara Sea. Mar. Geol. 190, S0025-3227(02)00347-X.

Kennett, J.P., Srinivasan, M.S., 1983. Neogene Planktonic Foraminifera: A Phylogenetic Atlas. Hutchinson Ross Publ., Stroudsburg, PA, 265 pp.

Kleijne, A., 1993. Morphology, Taxonomy and Distribution of Extant Coccolithophorids (Calcareous Nannoplankton). Drukkerij FEBA B.V., Enschede, 321 pp.

Kukal, Z., 1971. Geology of Recent Sediments. Academic Press, London, 490 pp.

Lane-Serff, G., Rohling, E.J., Bryden, H.L., Charnock, H., 1997. Post glacial connection of the Black Sea to the Mediterranean and its relation to the timing of sapropel formation. Paleoceanography 12, 169–174.

Latif, M.L., Özsoy, E., Salihoğlu, I., Gaines, A.F., Baştürk, Ö., Yilmaz, A., Tuğrul, S., 1992. Monitoring via Direct Measurements of the Modes of Mixing and Transport of Wastewater Discharges into the Bosphorus Underflow. Middle East Technical University, Institute of Marine Sciences, Tech. Rep. 92-2, 98 pp.

MacDonald, J.C., 2000. Quaternary palaeoecology of molluscs from the Marmara and Black Seas. Honours B.Sc. Dissertation. Memorial University of Newfoundland, St. John's, NF, 90 pp.

Mastel, R., 1997. Noah's flood. New Sci. 156, 24–27.

McInnis, D., 1998. Two geologists trace Noah's Flood to the violent birth of the Black Sea. Earth (August), 46–54.

Mordukhai-Boltovskoi, F.D., 1972. Keys for Identification of Fauna of the Black and Azov Seas (Opredelitel Fauny Chernogo I Azovshkogo Morej), Volume 3: Free Living Invertebrates (in Russian). Naukova Dumka, Kiev, 339 pp.

Mudie, P.J., Aksu, A.E., Yaşar, D., 2001. Late Quaternary dinoflagellate cysts from the Black, Marmara and Aegean seas: variations in assemblages, morphology and paleosalinity. Mar. Micropaleontol. 43, 155–178.

Mudie, P.J., Rochon, A., Aksu, A.E., Gillespie, H., 2002a. Dinoflagellate cysts, freshwater algae and fungal spores as salinity indicators in Late Quaternary cores from Marmara and Black Seas. Mar. Geol. 190, S0025-3227(02)00348-1.

Mudie, P.J., Rochon, A., Aksu, A.E., 2002b. Pollen stratigraphy of Late Quaternary cores from Marmara Sea: land–sea correlation and paleoclimatic history. Mar. Geol. 190, S0025-3227(02)00349-3.

Oktay, F.Y., Gökaşan, E., Sakınç, M., Yaltırak, C., Imren, C., Demirbağ, E., 2002. The effects of the North Anatolian Fault Zone to the latest connection between Black Sea and Sea of Marmara. Mar. Geol. 190, S0025-3227 (01)00246-8.

Özsoy, E., Latif, M.A., Tuğrul, S., Ünlüata, Ü., 1995. Exchanges with the Mediterranean, fluxes and boundary mixing processes in the Black Sea. In: Briand, F. (Ed.), Mediterranean Tributary Seas. Bulletin de l'Institut Océanographique Monaco, Special No. 15, CIESME Science Series, 1, pp. 1–25.

Pfannenstiel, M., 1944. Diluviale Geologie des Mittelmeergebietes die Diluvialen Entwicklundgstadien und die Urgeschite von Dardanellen, Marmara Meer und Bosphorus. Geol. Rundsch. 34, 334–342.

Polat, Ç., Tuğrul, S., 1996. Chemical exchange between the Mediterranean and Black Sea via the Turkish Straits. In: Briand, F. (Ed.), Dynamics of Mediterranean Straits and Channels. Bulletin de l'Institut Océanographique Monaco, Special No. 17, CIESME Science Series 2, pp. 167–186.

Poppe, G.T., Goto, Y., 1991. European Seashells, Vol. I. Verlag Christa Hemmen, Wiesbaden, 352 pp.

Poppe, G.T., Goto, Y., 1993. European Seashells, Vol. II. Verlag Christa Hemmen, Wiesbaden, 221 pp.

Ryan, W.B.F., Pitman, W.C., III, 1998. Noah's Flood. Simon and Schuster, New York, 319 pp.

Ryan, W.B.F., Pitman, W.C., III, Major, C.O., Shimkus, K., Maskalenko, V., Jones, G.A., Dimitrov, P., Görür, N., Sakınç, M., Yüce, H., 1997. An abrupt drowning of the Black Sea shelf. Mar. Geol. 138, 119–126.

Saito, T., Thompson, P.R., Berger, D., 1981. Systematic Index of Recent and Pleistocene Planktonic Foraminifera. University of Tokyo Press, 190 pp.

Skene, K.I., Piper, D.J.W., Aksu, A.E., Syvitski, J.P.M., 1998. Evaluation of the global oxygen isotope curve as a proxy for Quaternary sea level by modeling of delta progradation. J. Sediment. Res. 68, 1077–1092.

Smith, A.D., Taymaz, T., Oktay, F., Yüce, H., Alpar, B., Başaran, H., Jackson, J.A., Kara, S., Şimşek, M., 1995. High-resolution seismic profiling in the Sea of Marmara (northwest Turkey): late Quaternary sedimentation and sea-level changes. Geol. Soc. Am. Bull. 107, 923–936.

Stuiver, M., Reimer, P.J., Bard, E., Beck, J.W., Burr, G.S., Hughen, K.A., Kromer, B., McCormac, G., van der Plicht, J., Spurk, M., 1998a. INTCAL98 radiocarbon age calibration, 24000–0 cal BP. Radiocarbon 40, 1041–1083.

Stuiver, M., Reimer, P.J., Braziunas, T.F., 1998b. High-precision radiocarbon age calibration for terrestrial and marine samples. Radiocarbon 40, 1127–1151.

Winter, A., Siesser, W., 1994. Coccolithophores. Cambridge University Press, 242 pp.

Yaltırak, C., Sakınç, M., Aksu, A.E., Hiscott, R.N., Galleb, B., Ülgen, U.B., 2002. Late Pleistocene uplift history along the southwestern Marmara Sea determined from raised coastal deposits and global sea-level variations. Mar. Geol. 192, S0025-3227(02)00351-1.

Yim, W.W.-S., 1999. Radiocarbon dating and the reconstruction of late Quaternary sea-level changes in Hong Kong. Quat. Int. 55, 77–91.